Pure and Applied Geophysics

Supporting Information for

Spectral Characterization of Coastal Tsunami Response in Suruga Bay, Japan, Using Stochastic Simulation Ensembles

Takuya Miyashita[1], Tung-Cheng Ho[1], Nobuhito Mori[1,2,3], Tomoya Shimura[1]

[1] Disaster Prevention Research Institute, Kyoto University, Kyoto, Japan.
[2] Typhoon Research Center, Yokohama National University, Kanagawa, Japan.
[3] School of Engineering, Swansea University, Swansea, UK.

Contents of this file

Introduction

The following figures show additional detailed information on the stochastic source model, numerical setup, consistency on the response function, and comparison of simulated and observed waveforms. All of the synthetic finite fault models that allow to replicate these results have been uploaded to Zenodo: https://doi.org/10.5281/zenodo.15845359

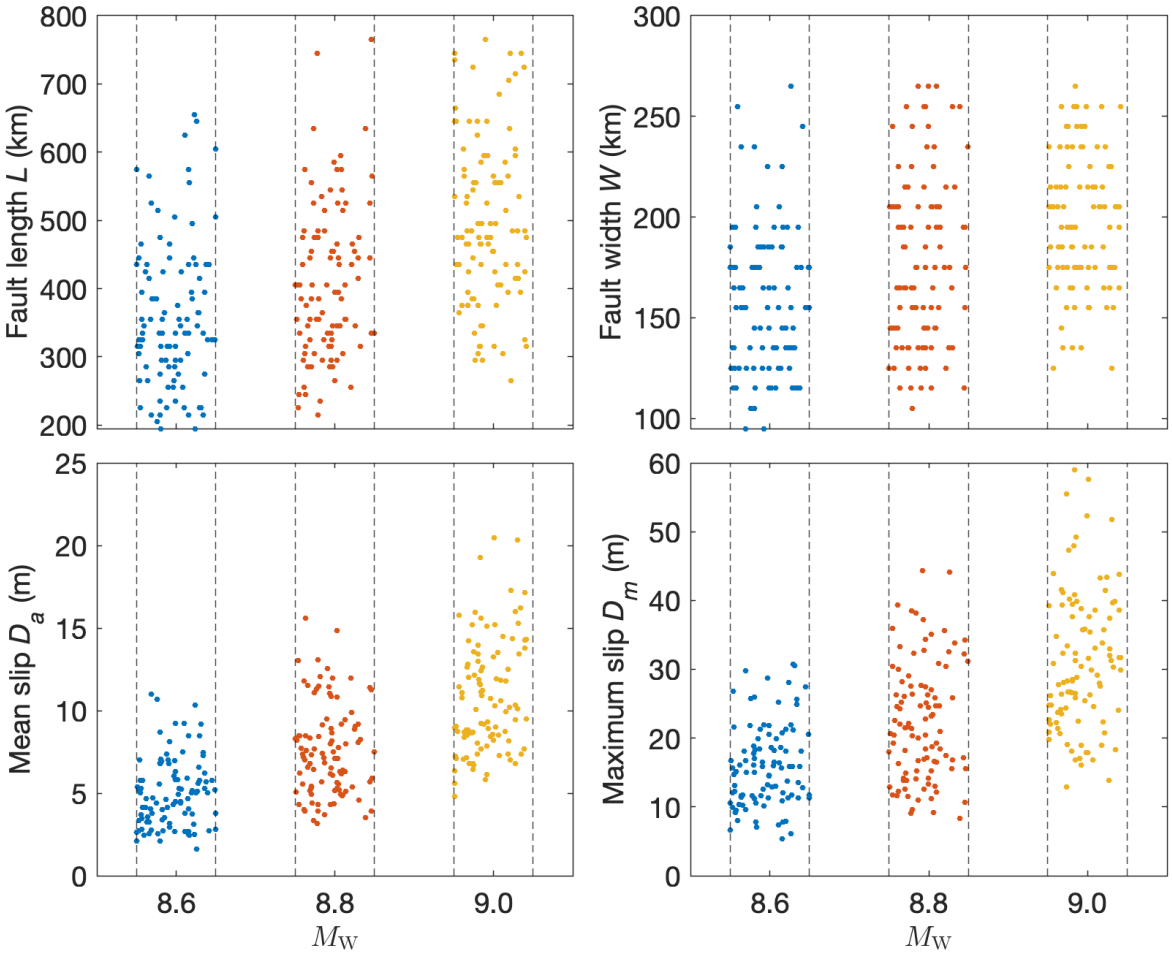

Figure S1. Key source parameters for the 300 fault models generated. Each panel shows the fault width, fault length, mean slip, and maximum slip. Three patterns of magnitudes are targeted, with an allowable error of ±0.05.

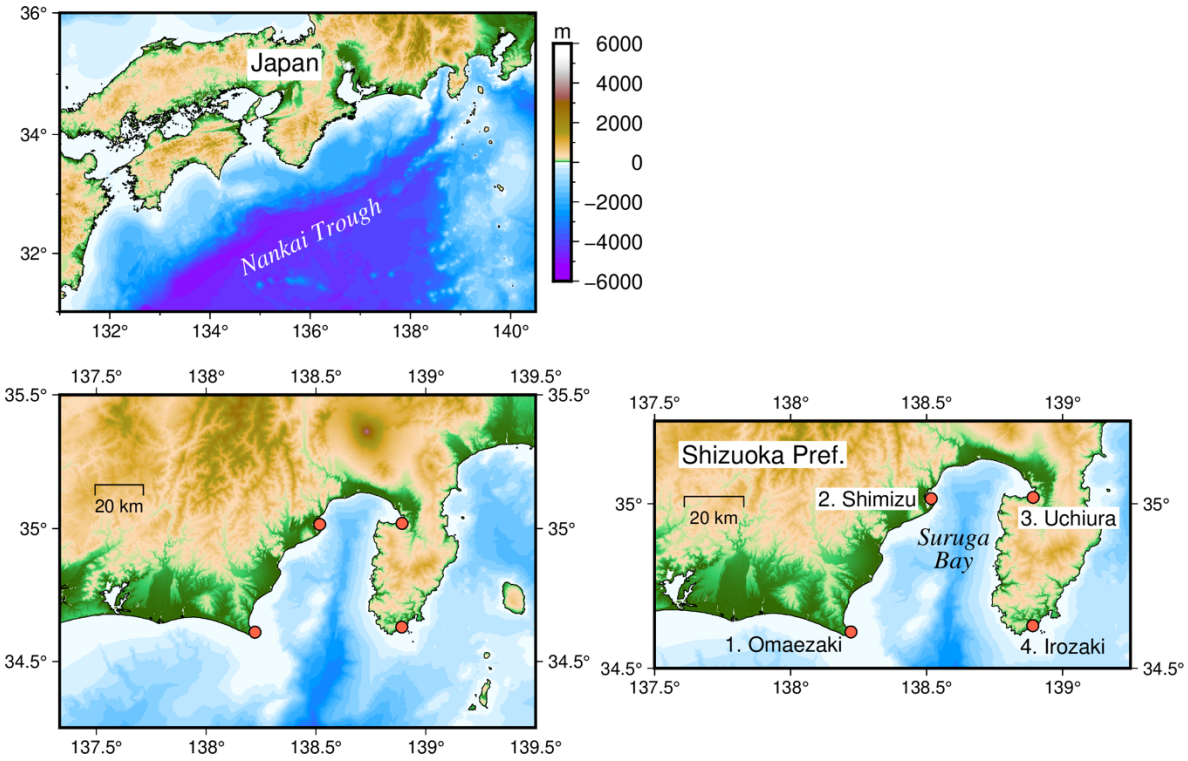

Figure S2. Bathymetry for numerical tsunami simulations. Each panel refers to a domain of nesting, with resolutions of 30, 10, and 10/3 arcseconds.

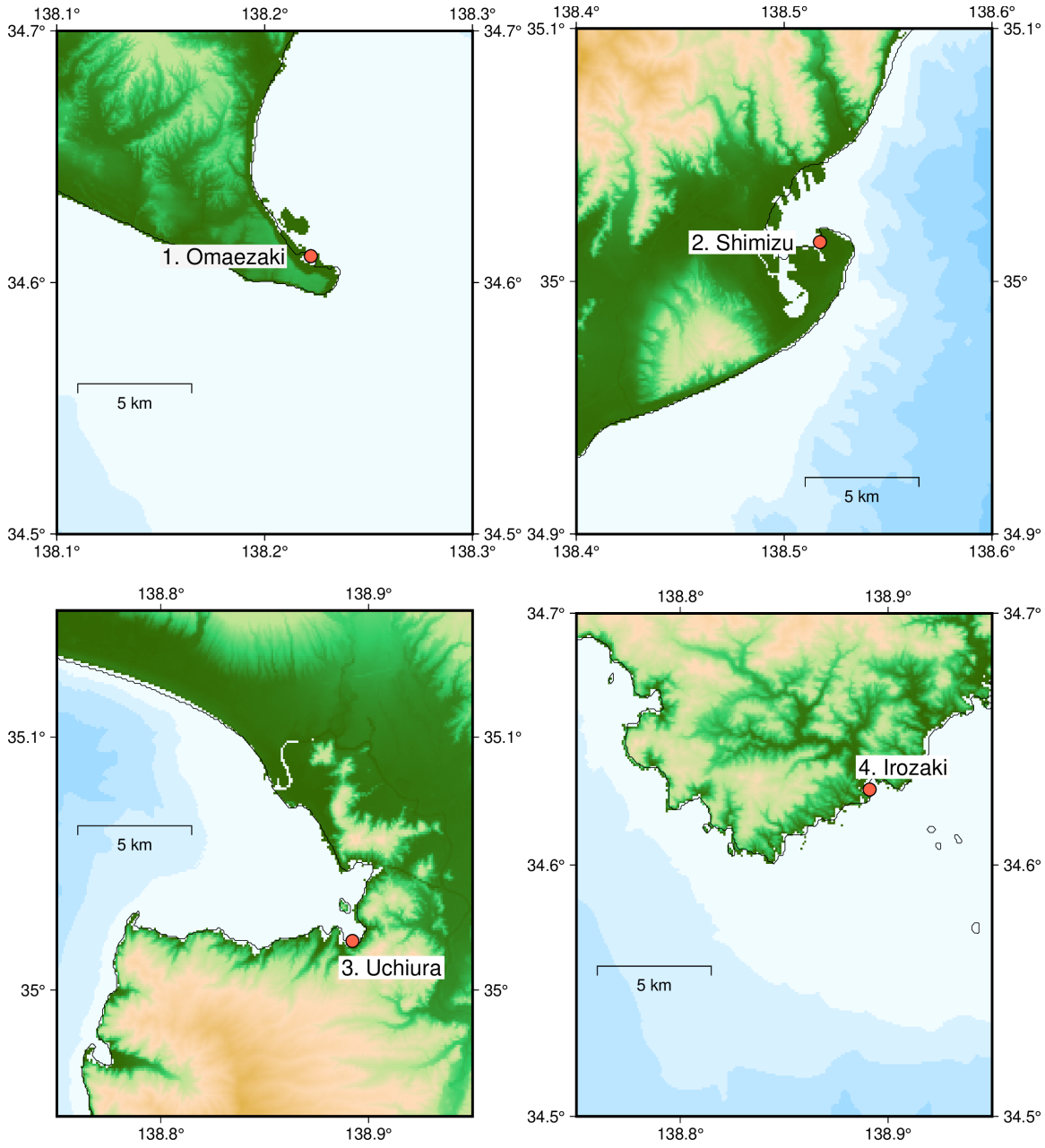

Figure S3. Enlarged maps of bathymetry around the four JMA tide gauges that are the focus of this study.

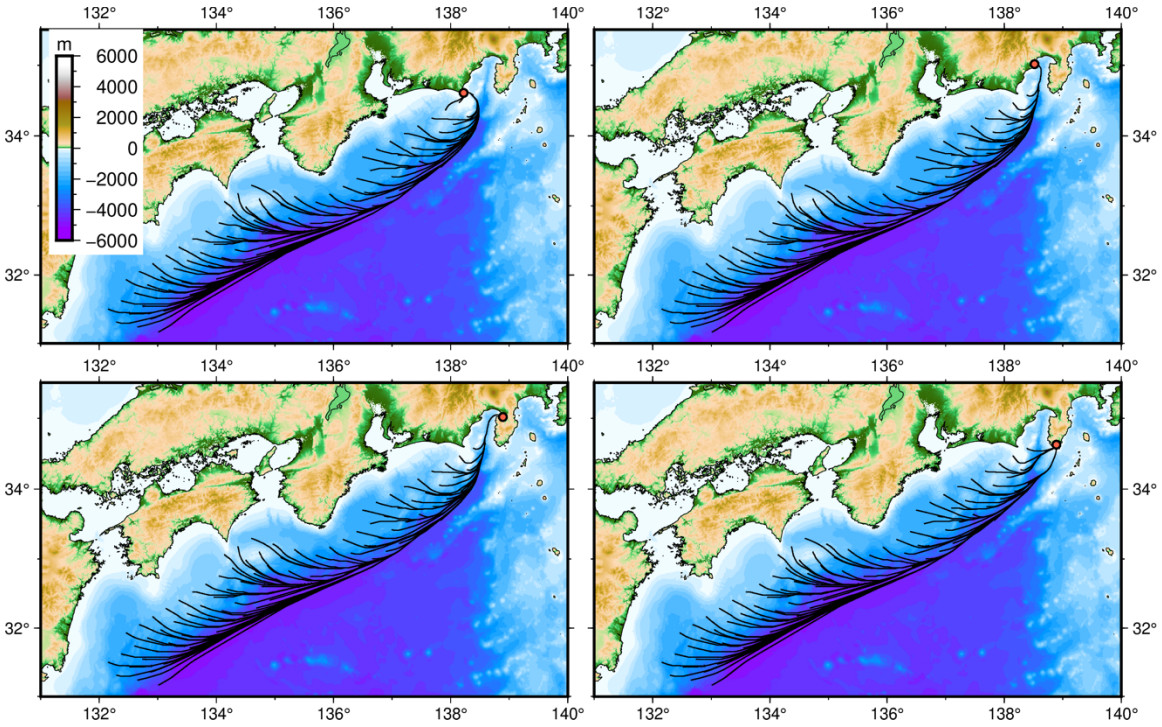

Figure S4. All tsunami ray paths from the source region to the coast obtained by the ray tracing method. 100 points are located in the source region and the paths to reach the 4 coastal gauges.

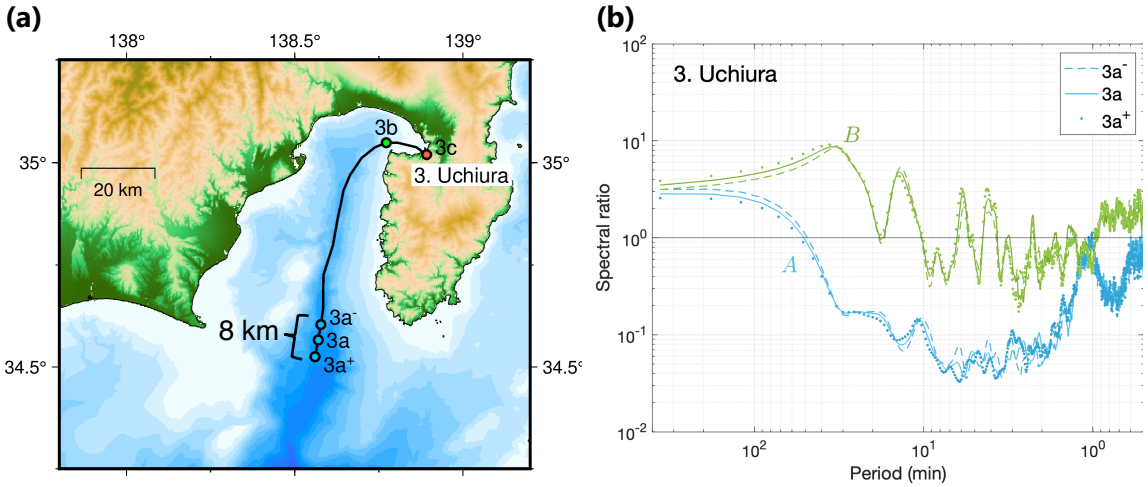

Figure S5. Sensitivity of the response function to different positions of the virtual gauge. (a) Difference in the position of the virtual gauge. It is slightly shifted on raypath from the original 3a location, and the distance between 3a- and 3a+ is about 8 km. (b) Comparison of response functions obtained using 3a-, 3a, and 3a+.

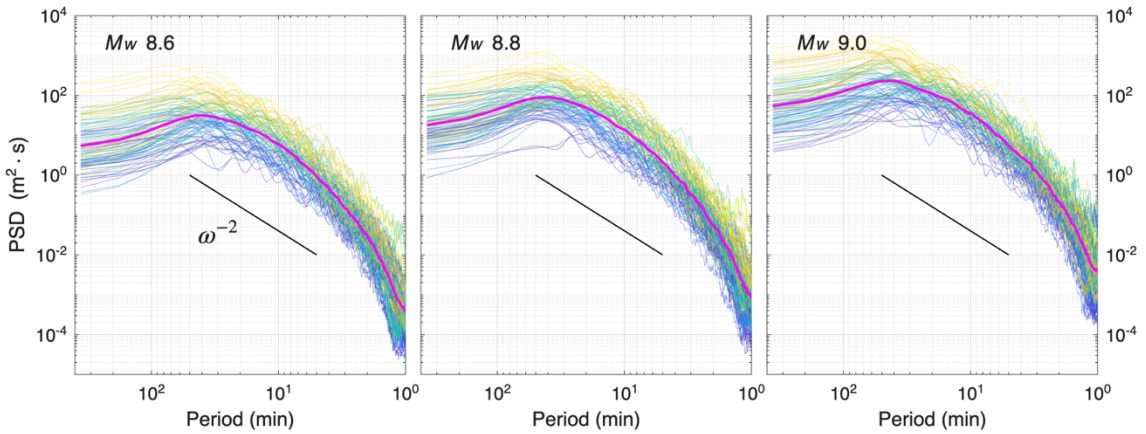

Figure S6. Source spectra of 300 tsunami scenarios obtained from tsunami simulations. From left to right, these correspond to moment magnitudes of 8.6, 8.8, and 9.0. The thick magenta lines represent the geometric mean of 100 source spectra for each magnitude.

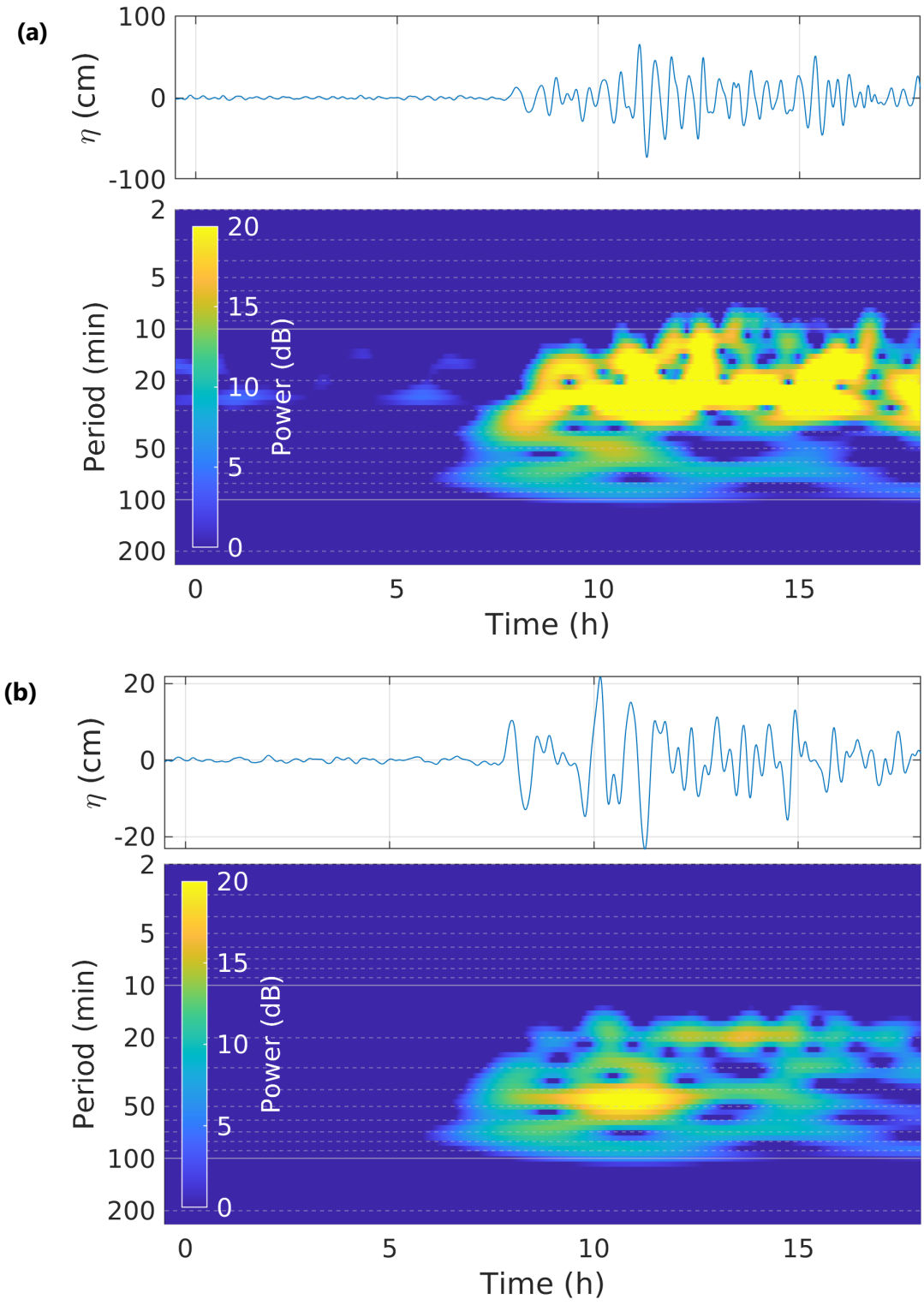

Figure S7. Wavelet analysis of the observed waveforms during the 2022 Tonga meteorological tsunami at four locations in this study, obtained by Miyashita et al. (2023). (a) 1. Omaezaki, (b) 2. Shimizu.

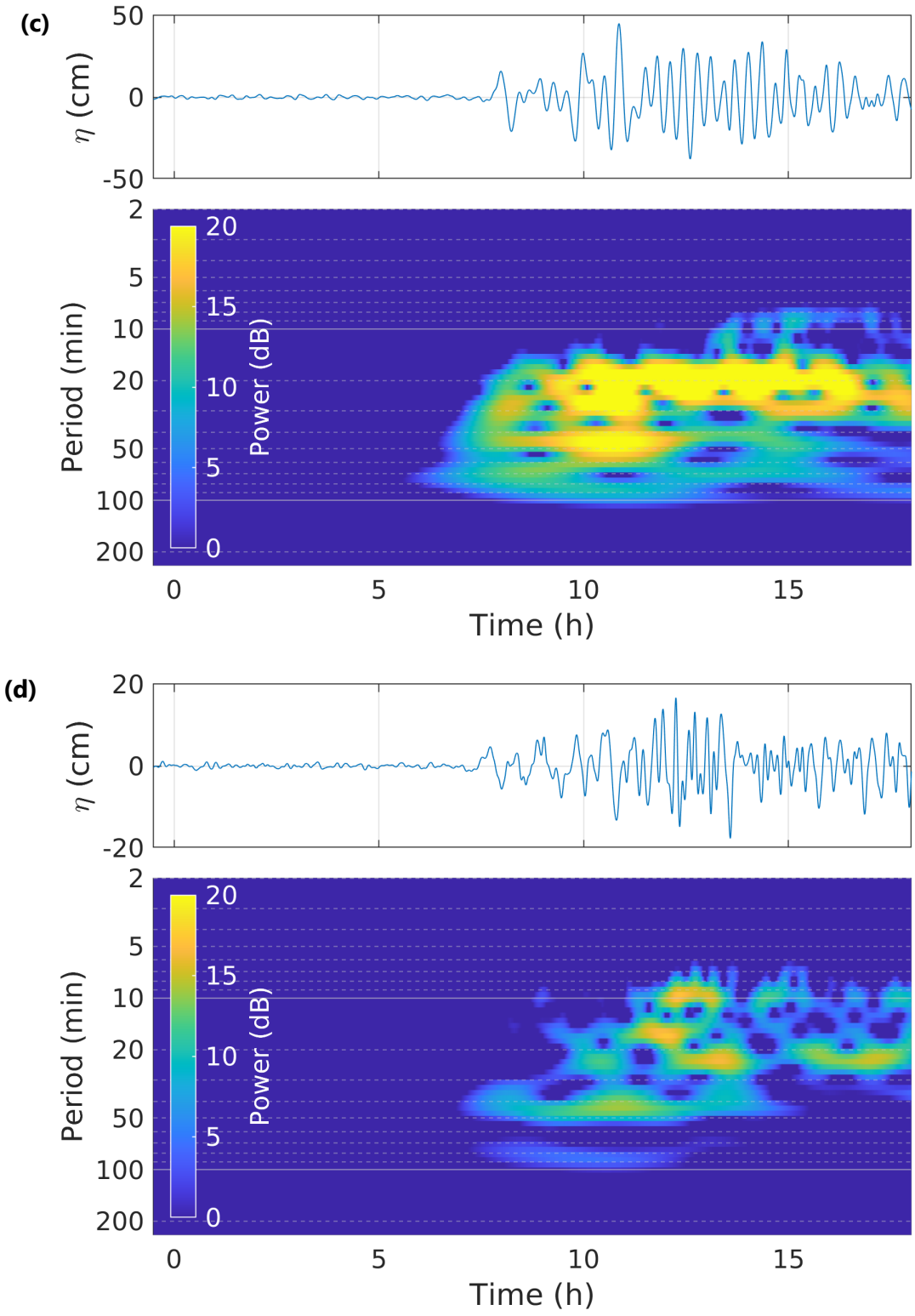

Figure S7. Continued: (c) 3. Uchiura and (d) 4. Irozaki

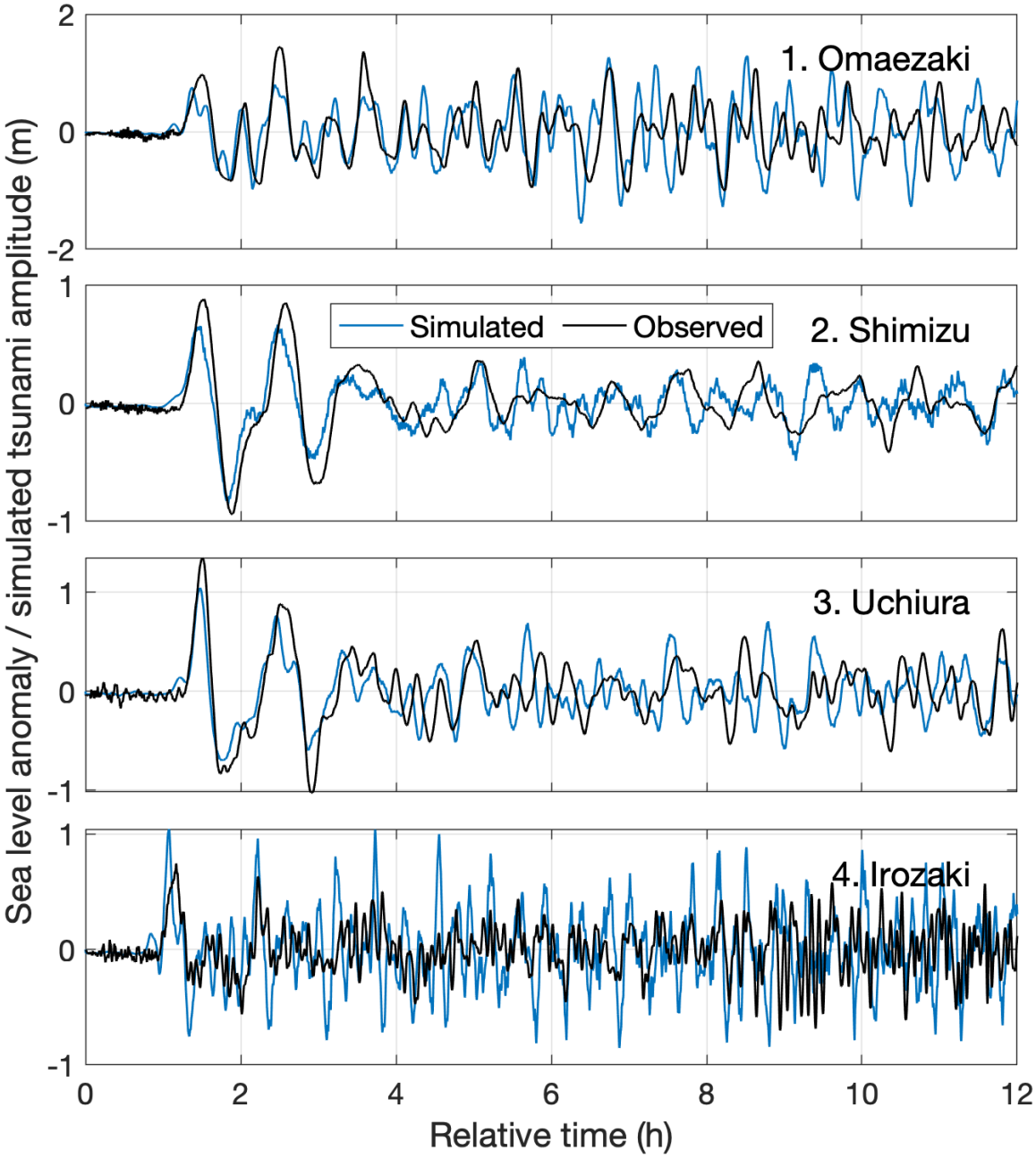

Figure S8. Observed tsunami waveform (black line) and computed one (blue line) using the source model of the 2011 Tohoku tsunami along the Suruga Bay coastal area. The source model used is as described in the main text.

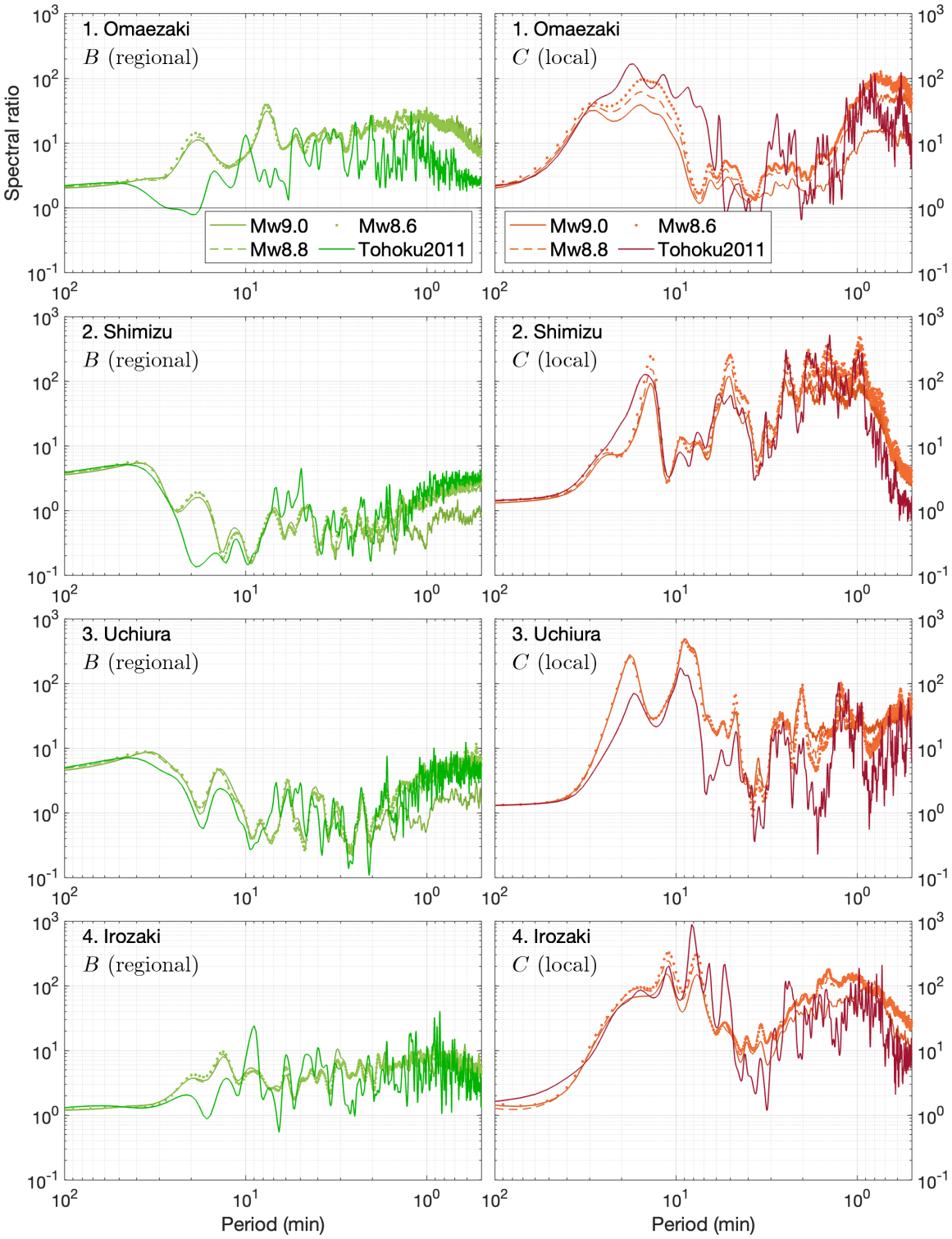

Figure S9. Comparison of response functions for different earthquake magnitudes and wave source areas. The left panel show regional response *B* and the right panel shows local response *C*. The difference in line type indicates either the magnitude difference or the 2011 Tohoku tsunami case.

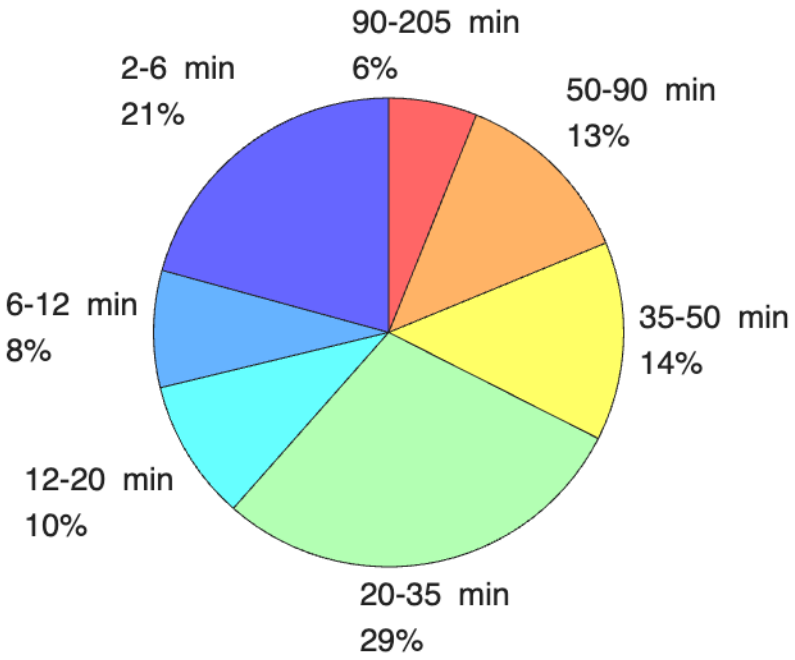

Figure S10. The energy contribution ratio calculated by integrating the source spectrum of the 2011 Tohoku tsunami divided into seven periodic bands. For comparison, the same periodic bands as Zaytsev et al. (2017) are used.

References

Miyashita, T., Nishino, A., Ho, T.-C., Yasuda, T., Mori, N., Shimura, T., & Fukui, N. (2023). Multi-scale simulation of subsequent tsunami waves in Japan excited by air pressure waves due to the 2022 Tonga volcanic eruption. *Pure and Applied Geophysics*, 180, 3195-3223.

Zaytsev, O., Rabinovich, A. B., & Thomson, R. E. (2017). The 2011 Tohoku tsunami on the coast of Mexico: A case study. *Pure and Applied Geophysics*, 174, 2961-2986.